Determination of loads and boundary conditions causing deformations of concentrating solar mirrors using non-derivative optimization methods and finite element analysis

Cite as: AIP Conference Proceedings **2303**, 160005 (2020); https://doi.org/10.1063/5.0029197
Published Online: 11 December 2020

Simon Schneider, Björn Schiricke, Eckhard Lüpfert, Andreas Reinholz, and Robert Pitz-Paal

Determination of Loads and Boundary Conditions Causing Deformations of Concentrating Solar Mirrors Using Non-Derivative Optimization Methods and Finite Element Analysis

Simon Schneider[1,3 b)], Björn Schiricke[1, a)], Eckhard Lüpfert[1], Andreas Reinholz[2, c)], Robert Pitz-Paal[1]

[1] *DLR German Aerospace Center, Solar Research, Linder Hoehe, 51147 Cologne, Germany*
[2] *AROpt-Consulting, Schmelzer Weg 8, 53844 Troisdorf, Germany*
[3] *Ibeo Automotive Systems GmbH, Merkurring 60-62, 22143 Hamburg, Germany*

[a)] Corresponding author: bjoern.schiricke@dlr.de
[b)] simon.s@posteo.de
[c)] andreas.reinholz@gmx.de

Abstract. Mirror shape optimization is a major part of improving the performance of concentrating solar power (CSP) collectors. Loads and boundary conditions of different origin and with varying influence on shape deviation need to be understood and quantified, e.g., in order to give specifications for the design of new collector generations. Finite element analysis (FEA) has proven to be a suitable method for evaluating mirror shape. An optimization process is presented that utilizes finite element models (FEM) of mirrors and a subsequent evaluation of the slope deviation to approximate a reference, e.g., a measured mirror shape, and determine the load values causing the mirror panel to deform. In this paper, the suggested approach is proven to be feasible: Two optimization algorithms are implemented: BOBYQA and CMA-ES. A simulated reference created in ANSYS Workbench and a reference from a deflectometry measurement are investigated. The determined geometrical parameters are compared to the reference values. For BOBYQA an absolute minimum and maximum deviation of 0.02 % and 0.3 %, and for CMA-ES of 0.0001 % and 0.004 % relative to the reference values is found. With the measured mirror shape as reference, the optimization algorithm was again capable of reproducing the mirror shape in FEA. However, the geometrical load parameters found were only partially in agreement with the measured values. Yet, it is concluded that the proposed method for reproducing mirror shape works.

INTRODUCTION

Various loads like wind, dead load, and forces originating from the subjacent support structure lead to shape deviations of the mirror panels when mounted on the collector frame. Moreover, the resulting shape accuracy depends on given boundary conditions, e.g., the tracking angle of the collector. Deformed mirrors can lower the optical efficiency of the collector due to a decreased intercept factor if reflected sun rays miss the receiver.

A parabolic trough collector for concentrating solar power is constructed so that the mirrors withstand occurring loads and maintain the ideal parabolic shape during operation in order to maximize the annual yield of the plant. With more than half a million individual mirror panels in a state-of-the-art CSP plant an economic collector design is mandatory to reach low investment costs and competitive electricity generation costs.

As stated by Giannuzzi et al. [1] the criteria for designing and developing new collector generations are: Safety (public protection when the collector is exposed to static load), Optical Performance (material stiffness high enough to avoid displacements and mirror shape deviations), Mechanical Functionality (e.g., allowing tracking without any colliding parts), and Low Cost (effective use of available on-site and material resources while maintaining safety

SolarPACES 2019
AIP Conf. Proc. 2303, 160005-1–160005-12; https://doi.org/10.1063/5.0029197
Published by AIP Publishing. 978-0-7354-4037-1/$30.00

requirements as stated above). Therefore, a trade-off between stiffness and stability on the one hand and an economic design on the other hand is mandatory. Influences on the mirror shape, e.g., those originating from the collector support structure need to be understood and their effects on mirror shape deviation need to be quantified. Specifying tolerances for manufacturing parameters and collector loads is made possible.

In previous works the influence of loads (dead-load, wind-load, type and stiffness of support structure) on the resulting mirror shape accuracy were evaluated and quantified [2]. In contrast, a typical scenario in reality is usually vice versa: The mirror shape accuracy is measured, e.g., with deflectometry [3], distant observer methods like TARMES [4] or QFly [5] or other methods like VSHOT [6],[7] while the loads causing the mirrors to deform are unknown or at least not exactly quantified. Therefore, it is somehow obvious to introduce a method with measured mirror shape data as input that is able to determine the loads and boundary conditions that led to the observed mirror shape.

In this paper, the suggested approach making use of optimization algorithms is proven to be feasible. The chosen method is presented and the developed algorithm is described. Eventually, comparisons with simulated data from finite element models (FEM) as well as with optical measurements carried out at the QUARZ laboratory at DLR, Cologne, using a real mirror of RP3 geometry, are presented and deviations discussed.

The work presented here was created during the doctorate of the first author, parts of the results found their way into the dissertation [8].

METHOD

Use of Finite Element Analysis and Optimization Algorithms in Solar Research

Finite element analysis has proven to be a suitable method for simulating solar collectors and predicting mechanical and optical properties under operating conditions. As presented by Geyer et al. the development of the EuroTrough collector was advanced by FE-analyses [9]: Structural investigations under different load cases were carried out and the optimal configuration was identified. Christian and Ho used FEA and a linking to ray tracing to determine the influence of gravity load and bending on the slope deviation of the mirror panels and eventually the impact on the intercept factor [10],[11]. Moya and Ho created finite Element Models of the heliostats at the National Solar Thermal Test Facility at Sandia National Laboratories in Albuquerque [12]. The effect of displacements in different load scenarios was investigated and compared to experimental results. A later study by Yuan, Christian, and Ho involved the Advanced Thermal Systems (ATS) heliostat [13]. Another presentation regarding the linking of FEM with ray tracing in form of a finite element ray tracer (FERT) was published by Biggio et al. in 2013 [14]. The advantage of including this type of analysis in the design process of new collector generations was pointed out. Gong et al. performed dynamic measurements at heliostats in order to identify modal parameters and characterize dynamic behavior [15]. A finite element model of the heliostat was updated with the obtained information in order to investigate the influence of wind-loads. Cheng et al. connected the Finite Volume Method (FVM) with Monte Carlo Ray Tracing (MCRT). The effect of geometric parameters of the parabolic trough system under investigation on the focus-shape was analyzed and eventually compared to the numerical FVM-MCRT-results obtained in simulations [16].

Optimization algorithms have previously been used in solar engineering. An overview regarding the application of optimization algorithms in the field of renewable and sustainable energy is given by Baños et al. [17]. The common approach is the parameterization of various components or even the whole plant. Those parameters are then optimized regarding maximum output values like power on the receiver or annual yield of the plant. Cabello et al. for example optimize the size of the plant, the thermal storage, and the power of the auxiliary system using to the annual profit as the objective function [18].

Husenbeth et al. linked the FEM software SOFiSTiK with the ray tracing tool CIRCE to automatically evaluate the incident power on the receiver for a mirror of a solar dish system [19]. The Matlab routine fminsearch was used to optimize the position of the mounting points relative to the inner and outer edges of the mirror. The inverse power was used as the objective function to be minimized.

The method presented in this paper differs in that not a characteristic of a certain component or a yield parameter of the whole system is optimized. Instead, a measured or simulated mirror shape is taken as reference and an attempt to reproduce this shape and reveal the causal load parameters is made.

The investigations conducted in this work are based on previous works by Meiser et al. [2], [20]-[23]: Finite element models of parabolic trough mirrors of RP3 geometry (as used in the EuroTrough collector) were developed.

Various loads and boundary conditions like dead load for different collector angles and the influence of different types of support structures (ideally-rigid substructure, elastic beam-substructure, and laboratory-frame) were investigated in structural-mechanical analyses in ANSYS Workbench. Based on the obtained deformation data the local slope deviation values of the mirror panel were calculated using a separate Matlab routine. A comparison with measured slope deviations obtained with the deflectometric test bench at DLR, Cologne was performed.

GENERAL WORKFLOW

An automatic workflow was developed within the scope of this work. A schematic overview is shown in Fig. 1: An initial set of parameters (starting values) is read from a spreadsheet by a Matlab routine and passed to a Finite element model of the solar mirror including various parts of the mirror mounting elements depending on the chosen optimization model. A structural-mechanical analysis is performed in ANSYS Workbench or ANSYS Mechanical APDL evaluating the influence of the given loads/parameters on the displacements of the discrete FE-nodes. The coordinates of the undeformed nodes as well as the associated displacements for the mirror are exported using an APDL macro. The data file is imported automatically into Matlab. Spatially resolved slope deviation values defining the mirror shape accuracy are derived. For the subsequent comparison with local slope deviation values of the reference (e.g., measured data), inaccuracies of the mirror material due to the manufacturing process are added to the FEM data: In order to minimize gravitational and mounting forces on the mirror and only measure the desired manufacturing errors, the mirror was positioned vertically during shape measurement with curved direction aligned with the horizon and the mirror in loose fixation. Hence, externally induced deformations were avoided.

The selected optimization algorithm decides whether the optimization process is continued with adjusted input parameters (loads) or ended in case any criterion of interruption is reached. The optimization algorithm itself is implemented either in Matlab script language or compiled for Matlab from other programming languages, e.g., C++.

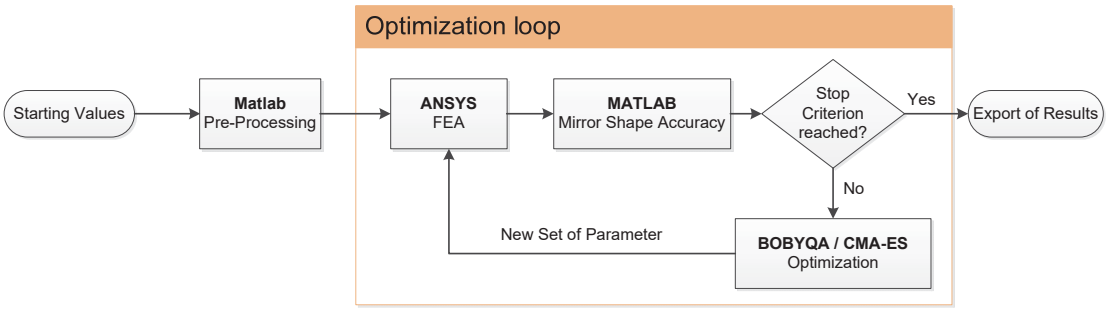

FIGURE 1. Schematic depiction of the workflow used for the optimization process employing BOBYQA or CMA-ES and FEA

Optimization Algorithms

Two different optimization algorithms were implemented and tested regarding applicability to the problem, accuracy of results and speed of convergence: CMA-ES and BOBYQA.

As an evolutionary algorithm, **CMA-ES** (Covariance Matrix Adaption - Evolutionary Strategy) makes use of selection, recombination, and/or mutation of current individuals (here: individual mirror shape results and their causal loads) to create a new generation of solutions with possibly less deviation from the reference case. It was introduced by Hansen and Ostermeier in 1996 [24] and is based on an adaptive approximation of the Hessian matrix. Although, as with most evolutionary algorithms, no proof of convergence exists, a robust optimization process and solution finding was expected. One iteration step includes multiple function evaluations (=multiple evaluations of the finite element model). For creating the new generation, two different combination strategies are applicable: With the comma-strategy only the individuals of the previous generation are used while the plus strategy takes into account all generations and results calculated. The latter strategy usually results in an improved focusing of the optimization procedure and is therefore used for the CMA-ES results presented in this work. For the simulated reference data, an initial stepsize $\sigma = 12$ was defined. Further information about CMA-ES can be found in [25]-[28].

The **BOBYQA** (Bound Optimization BY Quadratic Approximation) algorithm was introduced by Powell in 2009 [29]. It is derivative-free and therefore suitable for the optimization process including FEA in ANSYS.

BOBYQA makes use of a trust region solution strategy: A local quadratic model of the objective function is approximated within a pre-defined radius in parameter space and then minimized within this trust region. Before the actual optimization process, the quadratic model used for optimization is built by performing *2k+1* function evaluations with *k* as the number of optimization parameter. For the simulated reference, an initial trust region radius of $\rho_{start} = 10$ and a final radius of $\rho_{end} = 10^{-100}$ were set. For the measured reference, an initial trust region radius of $\rho_{start} = 90$ and a final radius of $\rho_{end} = 10^{-100}$ were set.

Description of FE-Model and Parameters Used for Optimization

Two finite element models consisting of single mirror panels of RP3 geometry (inner or outer mirror as part of parabolic trough collectors of EuroTrough geometry) originally designed by Meiser for previous works [20] were prepared, see Fig. 2. Parabolic mirrors with a thickness of 4 mm and a focal length of 1.71 m are modeled. All material properties of float glass with respect to static structural analyses were applied. Both models included the four cylindric-elliptical ceramic pads glued to the rear-side of the mirrors with silicone adhesive that allow the mirror mounting on the collector support structure. Solid elements were used for the discrete mesh. The mirror is divided into *n x n* elements with n = 200 as set by Meiser based on results of a convergence study [2]. For testing purposes, less elements were used (e.g., n = 50) in order to increase evaluation speed for a single optimization run.

The first model (*Pad model*) did not include further mounting elements or bodies, see Fig. 3 (a). External displacements on the rear sides of the mounting pads simulate effects originating from the subjacent bodies not included in the model. Translations as well as rotations around the coordinate system axes were allowed and parameterized in order to be used as optimization parameters addressed externally by the developed Matlab routines.

The second model (*Bracket model*) additionally included the L- and Z-brackets that served as linking elements between mirror mounting pads and the further substructure, more precisely the cantilever arms of the EuroTrough collector, see Fig. 3 (b). They were fixed to the rear side of the ceramic pads using bonded connections. No screws or other connecting elements were included in the model.

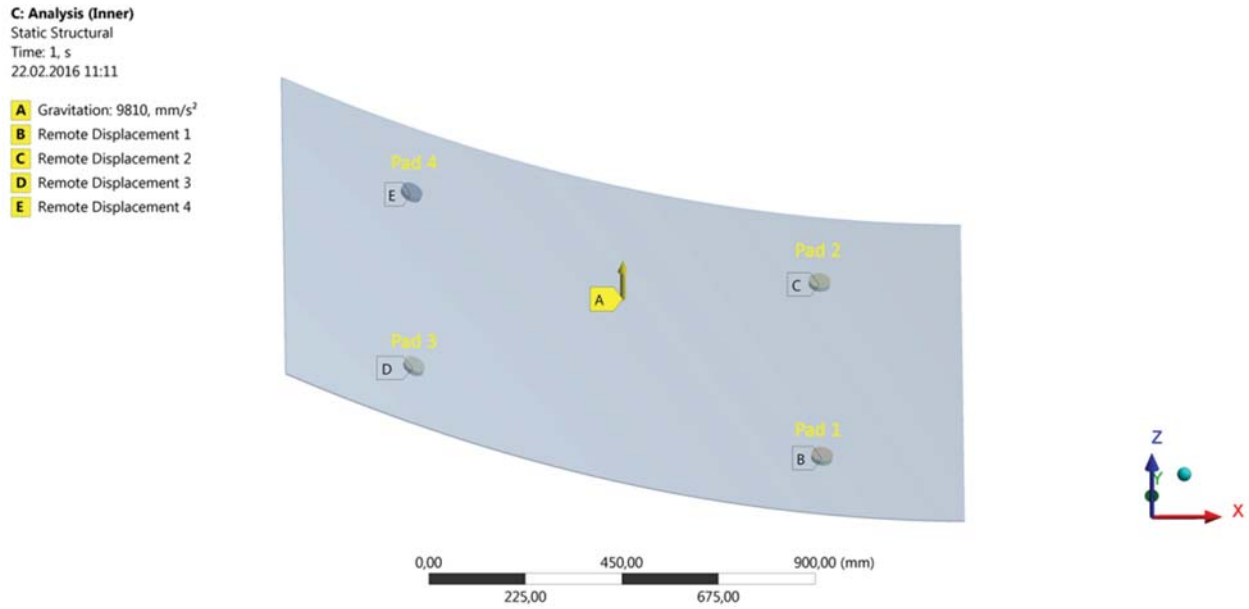

FIGURE 2. Finite element model of a parabolic trough inner mirror of RP3 geometry with mounting points 1 to 4

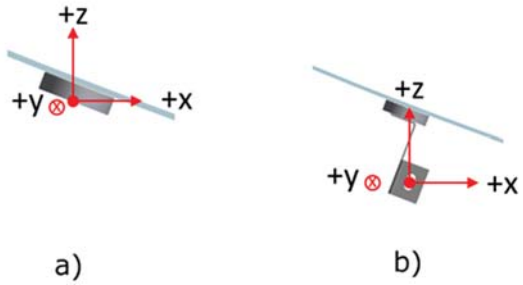

FIGURE 3. Depiction of the mounting elements included in the a) Pad model and b) Bracket model

In order to avoid non-unique solutions due to homogeneity of space (translations of all four mounting points and the whole mirror in the same direction), the translations of the lower right pad (=pad 1) were set to zero. This also decreased the number of parameters to be optimized. A separate column in the parameters spreadsheet allowed individual on/off switching for each parameter, deciding whether it was part of the optimization process or not. For instance, since the direction of gravitation was known, its components in x,y,z were not defined as optimization parameters.

Quantification of Mirror Shape Accuracy and Objective Function

External loads as well as material stresses from the manufacturing process create forces in the material that can lead to deviations from the ideal parabolic shape. Since the reflective layer or surface is also affected, these deviations also have an impact on the reflection quality of the mirror. This can be quantified by angular deviations of the surface normal vectors. Deviations in the *xz*-plane (defined by the curved dimension *x* of the trough and the upwards-direction *z* pointing from the vertex of the parabola to the focal point) directly affect the focus quality of the reflector. An outward rotation of the vector compared to its ideal direction is defined as a positive slope deviation and an inward rotation as a negative slope deviation. The slope deviation rms value SDx allows the characterization of a mirror panel by a single value [30]:

$$SDx = \sqrt{\sum_k \left(sdx_k^2 \cdot \frac{a_k}{A_{tot}} \right)} \qquad 1)$$

with the local slope deviation value sdx_k, the corresponding surface element area a_k, and the total aperture area A_{tot} of the mirror panel.

Comparisons between two mirror panels regarding shape accuracy were performed by taking the difference of slope deviation values. This can either be done by subtracting their SDx values each given by (1) or by calculating the sum of the differences of the local slope deviation values:

$$\Delta sdx = \sqrt{\sum_k \left(\left(sdx_{2,k} - sdx_{1,k} \right)^2 \cdot \frac{a_k}{A_{tot}} \right)} \qquad 2)$$

A value of zero would only result if all local slope deviation values $sdx_{2,k}$ and $sdx_{1,k}$ were identical. Hence, equation 2 was ideally suited and therefore used as the objective function for the optimization process.

Reference Case 1: Finite Element Model (Simulation)

In order to test the developed optimization method, simulated data of mirror shape deviations was created using the FE-models described above applying known external displacements to the mirror mounting elements. Induced mirror mounting deformations from ideal were 1 mm for translational deviations and 5 or 10 mrad for rotational deviations. These magnitudes correspond to values measured in production line, e.g. by Pottler et al. [31]. An optimization using the same FE-model (but without applying the displacements) was then employed until the objective function was minimized and a stop criterion met by the algorithm. The final (=best) set of parameters for the external displacements were compared to the applied known displacements of the reference case. Convergence speed and accuracy of the algorithms were assessed. For this reference case, the Pad model was employed.

Reference Case 2: Deflectometry & Photogrammetry (Real Measurement)

For testing the feasibility of applying the developed optimization method to actual mirror shape data, real mirrors of RP3 geometry were mounted on a laboratory support structure consisting of two original Euro Trough cantilever arms and a subjacent torque-box like metal frame, see Fig. 4. The L- and Z- brackets used as mounting elements for the mirrors were installed with deviations from their ideal positions and angles on purpose in order to induce clear shape deviations in the mirrors. A photogrammetric measurement using orientation measurement adapters (OMAs, see Fig. 5) was performed in order to determine the positions and angles of the brackets. The outcome was used for comparison with the resulting final (=best) set of parameters found by the optimization process. A non-scaling fit between photogrammetric data and displacements found by the optimization algorithm was performed in order to assimilate differences due to the used coordinate systems (fixed in the optimization model at the zero point for pad 1). For this reference case, the *Bracket model* was employed in order to consider the elasticity of the mirror mounting brackets).

FIGURE 4. Real and CAD image of the laboratory structure employed for the performed deflectometry measurements of RP3 mirrors and the subsequent photogrammetry measurements of the glass brackets

FIGURE 5. Orientation measurement adapter (OMA) for determining the position and angular orientation of the L- and Z-brackets used for mounting mirrors of RP3 geometry in EuroTrough collectors

RESULTS

Simulated Reference Data

The results of an exemplary test case employing the FE-model of an RP3 inner mirror using only simulated reference data as input for the optimization process is shown in Table 1. A mesh resolution for the mirror of 100x100 elements was chosen to increase optimization- and convergence-speed. Nine preselected and hence exactly known displacements were applied to the mirror mounting elements and the reference mirror shape was determined, see graphic (1) in Table 1. A slope deviation rms value of SDx = 3.91 mrad resulted. The two subjacent rows in Table 1 show the final slope deviation obtained with BOBYQA and CMA-ES, respectively. Both algorithms found a SDx of 3.91 mrad. The spatially resolved differences between optimization result and reference values are depicted in graphics (3) and (5) of Table 1 with a changed color scale ranging from -1 mrad to +1 mrad. BOBYQA met a stop criterion with a value for the objective function of $\Delta sdx = 1.31 \cdot 10^{-3}$ mrad, CMA-ES stopped after the maximum number of function evaluations with a value of $\Delta sdx = 4.41 \cdot 10^{-9}$ mrad. In this example, CMA-ES converged in less iteration steps (approx. 450) when compared to BOBYQA (approx. 930). An objective function

value of $\Delta sdx = 10^{-2}$ mrad is reached by BOBYQA after around 85 minutes while CMA-ES needs around 450 min. The complete optimization process took 3 hours 11 mins, 50 secs for BOBYQA and 16 hours, 24 mins, 5 secs for CMA-ES until a stop criterion was met.

The individual convergences of the optimization parameters are shown in comparison in Fig. 6. BOBYQA uses the first $2k + 1 = 19$ function evaluations to build the quadratic model and then optimizes each parameter along a nearly continuous path until the stop criterion is met; CMA-ES scans the parameter space more discontinuously covering a broader area.

In summary, CMA-ES achieved a higher accuracy while BOBYQA reached the same objective function value in less time: For BOBYQA a minimum and maximum deviation of 0.02 % and 0.3 %, respectively, and for CMA-ES of 0.0001 % and 0.004 %, respectively, relative to the known defined values for the displacements of the simulated reference case were found.

TABLE 1. Resulting slope deviation values (in mrad) for the optimization process with simulated mirror shape data as reference for the BOBYQA- and CMA-ES algorithms in comparison

(1) Reference case SDx = 3.91 mrad 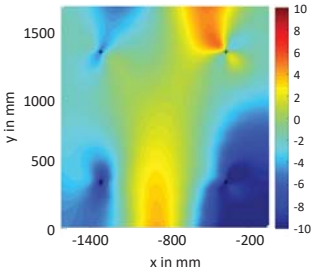	(2) BOBYQA FEM result SDx = 3.91 mrad 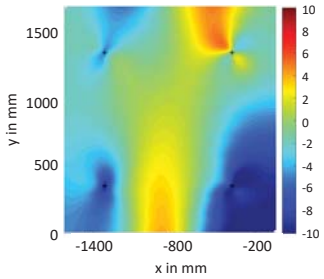	(3) Differences: BOBYQA FEM result to reference, equal to (2) - (1) Δ(sdx) = 1.31 E-3 mrad 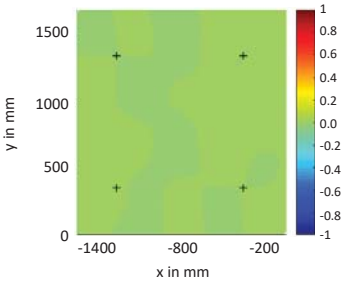
	(4) CMA-ES FEM result SDx = 3.91 mrad 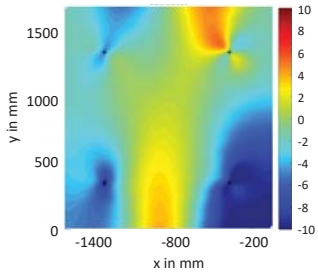	(5) Differences: CMA-ES FEM result to reference, equal to (4) - (1) Δ(sdx) = 4.41 E-9 mrad 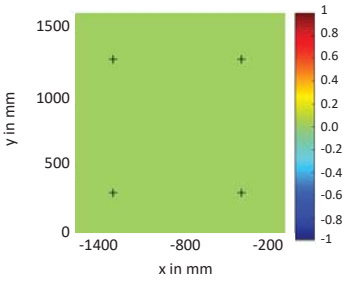

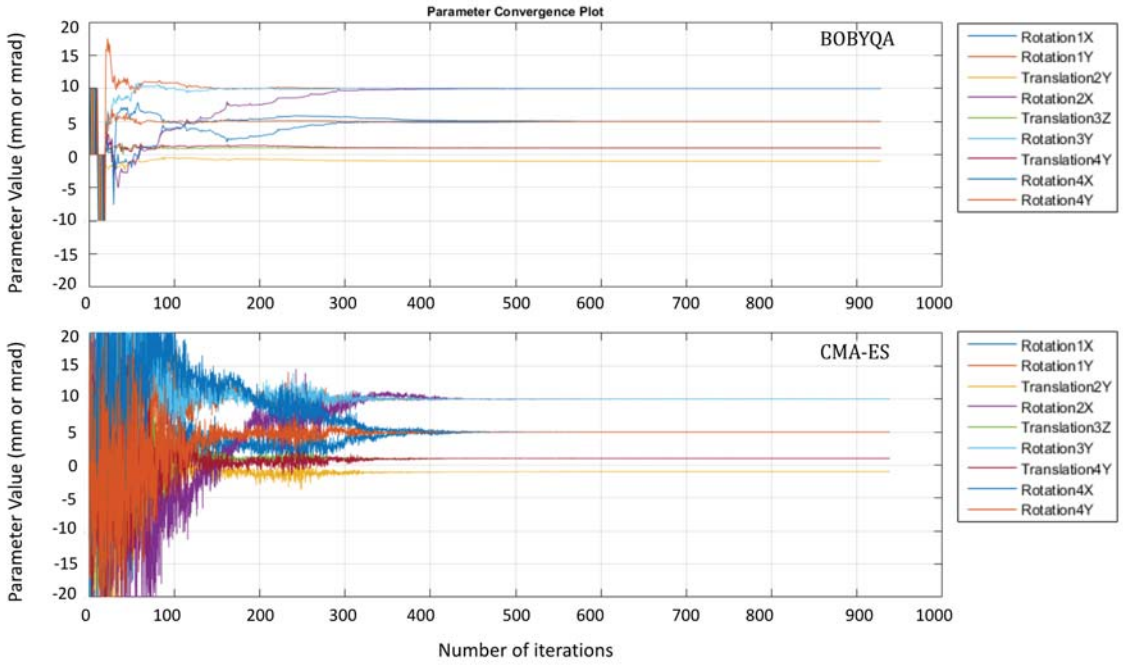

FIGURE 6. Parameter convergence plots against the number of iterations for the simulated data as reference for both algorithms: BOBYQA (upper graph) and CMA-ES algorithm (lower graph). Parameter values given in mrad for rotations and in mm for translations.

Real Deflectometric Measurement Data

Table 2 shows the results of applying the optimization process to real deflectometric measurement data of an RP3 inner mirror carried out at the QUARZ laboratory, DLR, Cologne. In graphic (1) the resulting slope deviation as measured with deflectometry is shown. A slope deviation rms value of SDx = 3.57 mrad was determined. In graphic (2) the slope deviation resulting from the FE-model is shown. The slope deviations caused by material stresses from the manufacturing process of the mirror are depicted in graphic (3). These were determined in the laboratory by measuring the mirror in as load-free a position as possible during the measurement. This corresponds to a vertical position of the mirror with the parabolically curved dimension along the horizon as well as with loose mounting, so that almost no or no relevant forces occur due to gravity or the mirror suspension. An SDx value of 2.40 mrad resulted. The BOBYQA result (FEM result from (2) with added material stress from (3)) is shown in graphic (4); corresponding spatially resolved slope deviation differences to the measured reference in (5). A slope deviation rms value of SDx = 3.55 mrad for the inner mirror is obtained by the algorithm. The final objective function value is $\Delta sdx = 0.38$ mrad.

An objective function value of approximately 0.5 mrad is attained after approximately 3 hours including the first 2k+1 function evaluations for building the quadratic model in the trust region. During the following 79 hours the improvement happened with a significantly lower rate until the optimization process was stopped by the algorithm. The parameter convergence against the number of iterations is presented in Fig. 7: translation parameters (upper diagram), rotation parameters (lower diagram). The initial values were set to zeros and no translations of the first mounting point were allowed. In order to make optimization and photogrammetry results comparable, both were individually fitted to the ideal values of the pad positions (lower side of the pads as shown in Fig. 3 a). Since ANSYS internally uses a special rotation convention, the photogrammetry results were post-processed to agree with this convention.

The measured mounting point deviations causing the real mirror shape deviations were in the order of a few mm for the translations and mrad for the rotations. The exact parameters determined with a photogrammetry measurement could not be reproduced in all cases, especially the rotational deviations of the brackets and the translational deviations in x- and y-direction. However, the z-deviation values agreed with relative deviations of -8% (bracket 1), -30% (bracket 2), -1% (bracket 3), and -59% (bracket 4).

TABLE 2. Resulting slope deviation values (in mrad) for the optimization process with simulated mirror shape data as reference for the BOBYQA- and CMA-ES algorithms in comparison

(1) Deflectometric measurement (with load) SDx = 3.57 mrad 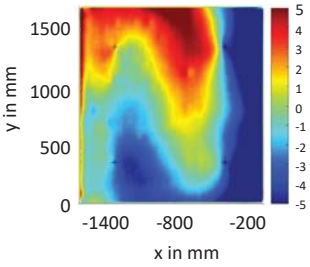	(2) BOBYQA optimization result (from FEM only), SDx = 2.39 mrad 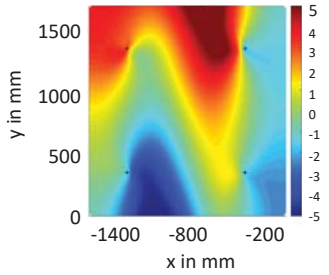	(3) Measured slope deviations caused by material stresses due to manufacturing (no load), SDx = 2.40 mrad 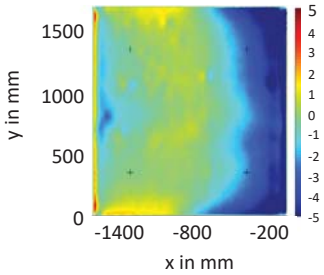
	(4) BOBYQA optimization result (FEM + from material stress), equal to (2) + (3), SDx = 3.55 mrad 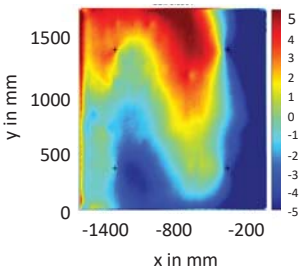	(5) Difference between optimization result and measurement (spatially-resolved, color scale = [-1,1]), equal to (4) - (1) 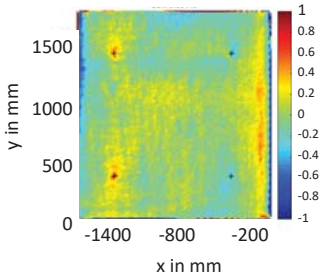

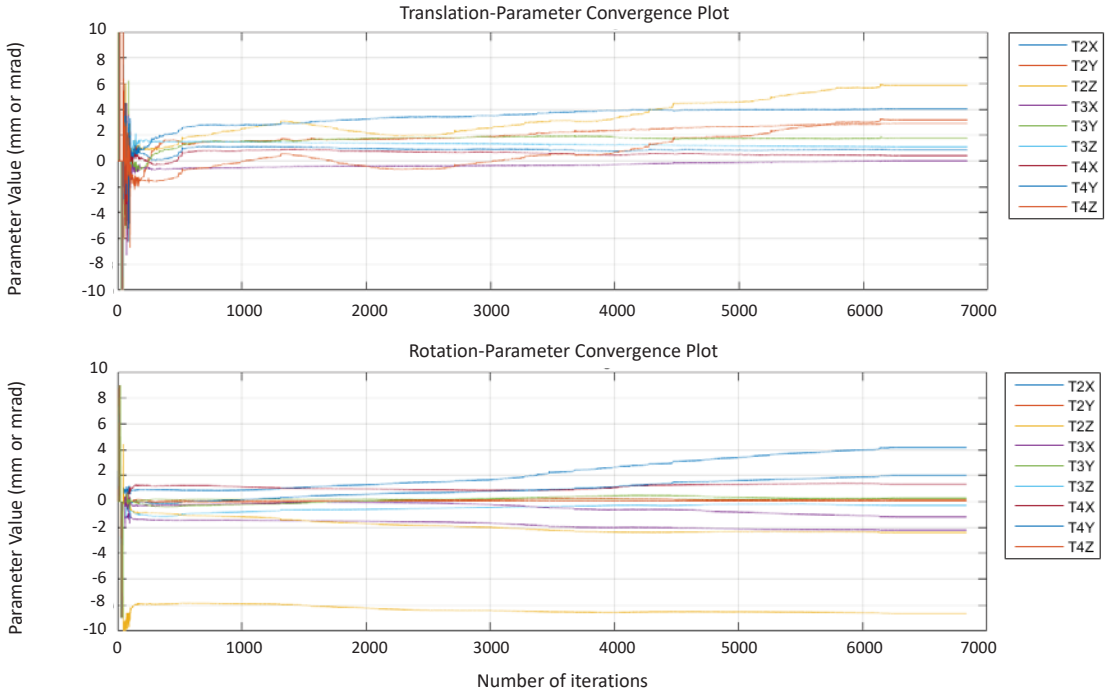

FIGURE 7. Parameter convergence plots showing the progress of the translations and rotations applied to the mounting elements of the inner mirror of RP3 geometry found by the BOBYQA algorithm (Note: y-axis limits of ±10 mm for translational parameters, ±100 mrad for rotational parameters)

DISCUSSION

The comparison of the two algorithms BOBYQA and CMA-ES using simulated mirror shape data and known displacement values as references proved that both algorithms were able to approximate the reference mirror shape and find the correct optimization parameters using zeros as starting values. However, for a single iteration step CMA-ES performs nine function evaluations each including a finite element analysis in ANSYS, while BOBYQA achieved the same accuracy (=value for the objective function) in less time. In the example presented, CMA-ES was able to find translational and rotational parameters with smaller relative deviation to the known reference values than BOBYQA. Considering that both algorithms achieved deviations from the reference values far less than 1 % as well as considering the amount of time required for the optimization, the BOBYQA algorithm was preferred for following and future evaluations.

For the measured slope deviation of the real mirror the presented optimization workflow was also capable of approximating the mirror shape. However, reproducing the mirror mounting point deviations did not work so well. One possible explanation is that a specific mirror shape may be caused by multiple different load configurations: The positions of the pads within the slot hole of the glass brackets differ from the ideal position (=mid of the slot hole) as soon as the brackets themselves show deviations from ideal. However, during the optimization run employing the finite element model, this was not a degree of freedom. Furthermore, in reality, the angular orientation of the pads relative to the bearing surface of the brackets might have differed from the ideal values (=coplanarity between pad rear side and bearing area of the brackets). Both effects were not covered by the employed state-of-the-art measurement technology and could have led to deviations in the obtained bracket positions and angles.

Summarizing the results for the real mirror, the data obtained by the performed optical measurement with the intention to characterize the real situation (loads and boundary conditions of the mirror mounting) was not sufficient for drawing a final conclusion whether the geometrical parameters found by the optimization algorithm were exactly those that lead to the measured mirror shape in reality.

As an attempt to discuss the presented method in a summarizing way regarding its validity, two aspects are emphasized: First, the underlying basic finite element model was already validated by Meiser using simulations and optical measurements [2] as well as re-validated by the author in the scope of this work and was therefore regarded as a trustworthy foundation for applying the presented algorithms. Second, the results presented above for reproducing simulated mirror shapes using well-known mounting deviations for the mirror resulted in high conformity for both mirror shape and mounting parameters: The applied geometrical deviations that were used to create the reference mirror shape were met with convincing accuracy.

In total – bearing in mind the results for simulation-only data and the limited knowledge of real mirror mounting deviations - it is stated that the proposed method works.

CONCLUSION

It is proven that measured mirror shape data can be approximated with simulations employing optimization algorithms and finite element analyses. With a reference created with the finite element model itself, and applied structural loads, both the mirror shape and the load values (geometrical deviations) were approximated with high accuracy.

Using a measured mirror shape and comparing the final set of load parameters to the ones obtained with an optical measurement, it was again possible to approximate the mirror shape. The obtained geometrical deviations causing the mirror to deform partly agreed with the measurements. As a reason for deviations, missing information that was not covered by state-of-the-art measurement techniques about the real situation regarding mirror mounting is assumed.

As an outcome of the study, factors influencing the mirror shape accuracy in solar thermal collectors can be better understood. The prediction of mirror shape accuracy in collector is improved. In accordance to the findings obtained in previous works the influence of the substructure on which the mirror is mounted significantly affects mirror shape accuracy. Even minor translational deviations in the range of millimeters or rotational deviations in the range of milliradians can have a significant effect on the overall shape of the mirror panel.

As yet, slope deviations caused by material stresses from the manufacturing process need to be measured, e.g., by deflectometry, and included in the optimization process. Future research shall address the question whether it is possible to leave out this additional step without losing accuracy in the determined load values. If this proves

successful, any mirror built in collector could be measured with regard to its shape and the optimization process responds with the underlying loads and boundary conditions. For good results within reasonable time, a fast optimization algorithm is required. By now, the time necessary for evaluating a single mirror panel is in the order of hours (approximately 2-20 hours, depending on the complexity of the FE-model, the computational performance, and the desired result accuracy). Therefore, a fast determination of load values is impossible, and, hence, a further speed improvement is desired.

For the optimization runs presented in this paper a starting vector of zeros was used. An educated guess based on mechanical knowledge or experience with mirror shape deviations is believed to improve evaluation speed and/or result accuracy. Further mirror shape data like the deviation in z (direction pointing from vertex of the parabola to the focal line) or the slope deviation in y may be consulted for the initial guess.

ACKNOWLEDGEMENT

The financial support for this work by the German Federal Ministry for Economic Affairs and Energy (BMWI) is gratefully acknowledged.

REFERENCES

1. G. M. Giannuzzi, C. E. Majorana, A. Miliozzi, V. A. Salomoni, and D. Nicolini, “Structural Design Criteria for Steel Components of Parabolic-Trough Solar Concentrators,” *J. Sol. Energy Eng.*, vol. 129, no. 4, p. 382, Nov. 2007.
2. S. Meiser, “Analysis of Parabolic Trough Concentrator Mirror Shape Accuracy in Laboratory and Collector”, Dissertation, RWTH Aachen University, 2013.
3. T. März, C. Prahl, S. Ulmer, S. Wilbert, and C. Weber, “Validation of Two Optical Measurement Methods for the Qualification of the Shape Accuracy of Mirror Panels for Concentrating Solar Systems,” *J. Sol. Energy Eng.*, vol. 133, no. 3, p. 31022, 2011.
4. S. Ulmer, K. Pottler, E. Lüpfert, and M. Röger, “Measurement Techniques for the Optical Quality Assessment of Parabolic Trough Collector Fields in Commercial Solar Power Plants,” *Proceedings of ES2007*. 01-Jun-2007.
5. C. Prahl, B. Stanicki, C. Hilgert, S. Ulmer, and M. Röger, “Airborne shape measurement of parabolic trough collector fields,” *Sol. Energy*, vol. 91, no. 0, pp. 68–78, May 2013.
6. S. A. Jones, D. R. Neal, J. K. Gruetzner, R. M. Houser, R. M. Edgar, J. Kent, and T. J. Wendelin, “VSHOT: A Tool for Characterizing Large, Imprecise Reflectors,” in *International Symposium on Optical Science Engineering and Instrumentation*, 1996.
7. S. A. Jones, J. K. Gruetzner, R. M. Houser, R. M. Edgar, and T. J. Wendelin, “VSHOT measurement uncertainty and experimental sensitivity study,” *Proc. 32nd Intersoc. Energy Convers. Eng. Conf.*, vol. 3, pp. 1877–1882, 1997.
8. S. Schneider, “Influences of Mirror Shape Accuracy on Performance Prediction for Parabolic Trough Concentrating Solar Power Systems”, Dissertation, RWTH Aachen University, 2017
9. M. Geyer, E. Lüpfert, R. Osuna, A. Esteban, W. Schiel, A. Schweitzer, E. Zarza, P. Nava, J. Langenkamp, and E. Mandelberg, “EuroTrough - Parabolic Trough Collector Developed for Cost Efficient Solar Power Generation,” in *Proceedings of the 11th Conference on Solar Power And Chemical Energy Systems (SolarPACES)*, 2002, pp. 1–7.
10. J. M. Christian and C. K. Ho, “Finite Element Modeling of Concentrating Solar Collectors for Evaluation of Gravity Loads, Bending, and Optical Characterization,” in *ASME 2010 4th International Conference on Energy Sustainability, Volume 2*, 2010, pp. 475–481.
11. J. M. Christian and C. K. Ho, “Finite Element Modeling and Ray Tracing of Parabolic Trough Collectors for Evaluation of Optical Intercept Factors With Gravity Loading,” in *ASME 2011 5th International Conference on Energy Sustainability, Parts A, B, and C*, 2011, pp. 577–585.
12. A. C. Moya and C. K. Ho, “Modeling and Validation of Heliostat Deformation Due to Static Loading,” in *Proceedings of the ASME 2011 5th International Conference on Energy Sustainability*, 2011, pp. 1–9.
13. J. K. Yuan, J. M. Christian, and C. K. Ho, “Compensation of Gravity Induced Heliostat Deflections for Improved Optical Performance,” *J. Sol. Energy Eng.*, vol. 137, no. 2, p. 21016, Nov. 2014.

14. K. Biggio, R. Backes, and J. Crawford, “Optical-Mechanical Analysis of Parabolic Trough Solar Concentrators to Support Commercial Development,” in *ASME 2013 7th International Conference on Energy Sustainability*, 2013.
15. B. Gong, Z. F. Wang, C. C. Zang, and Z. N. Li, “Model updating and structure optimization of heliostats based on vibration measurements,” in *Proceedings of the 21th Conference on Solar Power And Chemical Energy Systems (SolarPACES)*, 2015, vol. 0.
16. Z.-D. Cheng, Y.-L. He, K. Wang, B.-C. Du, and F. Q. Cui, “A detailed parameter study on the comprehensive characteristics and performance of a parabolic trough solar collector system,” *Appl. Therm. Eng.*, vol. 63, no. 1, pp. 278–289, Feb. 2014.
17. R. Baños, F. Manzano-Agugliaro, F. G. Montoya, C. Gil, A. Alcayde, and J. Gómez, “Optimization methods applied to renewable and sustainable energy: A review,” *Renew. Sustain. Energy Rev.*, vol. 15, no. 4, pp. 1753–1766, May 2011.
18. J. M. Cabello, J. M. Cejudo, M. Luque, F. Ruiz, K. Deb, and R. Tewari, “Optimization of the size of a solar thermal electricity plant by means of genetic algorithms,” *Renew. Energy*, vol. 36, no. 11, pp. 3146–3153, Nov. 2011.
19. C. Husenbeth, B. Zwingmann, and F. Von Reeken, “Optical and Structural Optimization by Linking FEM and Ray Tracing Analysis,” in *Proceedings of the 17th Conference on Solar Power And Chemical Energy Systems (SolarPACES)*, 2011.
20. S. Meiser, C. Kleine-Büning, R. Uhlig, E. Lüpfert, B. Schiricke, and R. Pitz-Paal, “Finite Element Modeling of Parabolic Trough Mirror Shape in Different Mirror Angles,” *J. Sol. Energy Eng.*, vol. 135, no. 3, p. 31006, Apr. 2013.
21. S. Meiser, E. Lüpfert, B. Schiricke, and R. Pitz-Paal, “Analysis of Parabolic Trough Concentrator Mirror Shape Accuracy in different Measurement Setups,” *Energy Procedia*, vol. 49, pp. 2135–2144, 2014.
22. S. Meiser, E. Lüpfert, B. Schiricke, and R. Pitz-Paal, “Conversion of parabolic trough mirror shape results measured in different laboratory setups,” *Sol. Energy*, vol. 111, pp. 396–406, Jan. 2015.
23. S. Meiser, S. Schneider, E. Lüpfert, B. Schiricke, and R. Pitz-Paal, “Evaluation and assessment of gravity load on mirror shape of parabolic trough solar collectors,” in *Proceedings of the 7th International Conference on Applied Energy - ICAE2015*, 2015, vol. 0.
24. N. Hansen and A. Ostermeier, “Adapting arbitrary normal mutation distributions in evolution strategies: the covariance matrix adaptation,” in *Proceedings of the IEEE Conference on Evolutionary Computation*, 1996, pp. 312–317.
25. N. Hansen and S. Kern, “Evaluating the CMA evolution strategy on multimodal test functions,” *Lect. Notes Comput. Sci. (including Subser. Lect. Notes Artif. Intell. Lect. Notes Bioinformatics)*, vol. 3242, pp. 282–291, 2004.
26. N. Hansen, *Towards a New Evolutionary Computation*, vol. 192. Berlin/Heidelberg: Springer-Verlag, 2006.
27. N. Hansen, “The CMA Evolution Strategy,” 2014. [Online]. Available: https://www.lri.fr/~hansen/cmaesintro.html. [Accessed: 22-Feb-2016].
28. P. Bayer and M. Finkel, “Optimization of concentration control by evolution strategies: Formulation, application, and assessment of remedial solutions,” *Water Resour. Res.*, vol. 43, no. 2, 2007.
29. M. J. D. Powell, “Cambridge Numerical Analysis Report NA2009/06, ‘The BOBYQA algorithm for bound constrained optimization without derivatives.’” Cambridge, England, 2009.
30. S. Ulmer, B. Heinz, K. Pottler, and E. Lüpfert, “Slope Error Measurements of Parabolic Troughs Using the Reflected Image of the Absorber Tube,” *J. Sol. Energy Eng.*, vol. 131, no. February, pp. 1–5, 2009.
31. K. Pottler, S. Ulmer, E. Lüpfert et al., "Ensuring performance by geometric quality control and specifications for parabolic trough solar fields", Energy Procedia 49 (2014), pp. 2170-2179